HHS Public Access

Author manuscript

Hepatology. Author manuscript; available in PMC 2020 November 01.

Published in final edited form as:

Hepatology. 2019 November ; 70(5): 1714–1731. doi:10.1002/hep.30700.

HIPPO SIGNALING CONTROLS NLRP3 ACTIVATION AND GOVERNS IMMUNOREGULATION OF MESENCHYMAL STEM CELLS IN MOUSE LIVER INJURY

Changyong Li[1,2], **Yuting Jin**[1], **Song Wei**[1], **Yishuang Sun**[2], **Longfeng Jiang**[1], **Qiang Zhu**[1], **Douglas G. Farmer**[1], **Ronald W. Busuttil**[1], **Jerzy W. Kupiec-Weglinski**[1], **Bibo Ke**[1]

[1]The Dumont-UCLA Transplant Center, Department of Surgery, David Geffen School of Medicine at UCLA, Los Angeles, CA, USA.

[2]Department of Physiology, School of Basic Medical Sciences, Wuhan University, Wuhan, China.

Abstract

The Hippo pathway, an evolutionarily conserved protein kinase cascade, tightly regulates cell growth and survival. Activation of yes-associated protein (YAP), a downstream effector of the Hippo pathway, has been shown to modulate tissue inflammation. However, it remains unknown as to whether and how the Hippo-YAP signaling may control NLRP3 activation in mesenchymal stem cell (MSC)-mediated immune regulation during liver inflammation. In a mouse model of ischemia/reperfusion (IR)-induced liver sterile inflammatory injury, we found that adoptive transfer of MSCs reduced hepatocellular damage, shifted macrophage polarization from M1 to M2 phenotype, and diminished inflammatory mediators. MSC treatment reduced MST½ and LATS1 phosphorylation but augmented YAP and β-catenin expression with increased PGE2 production in ischemic livers. However, disruption of myeloid YAP or β-catenin in MSC-transferred mice exacerbated IR-triggered liver inflammation, enhanced NLRP3/caspase-1 activity and reduced M2 macrophage phenotype. Using MSC/macrophage co-culture system, we found that MSCs increased macrophage YAP and β-catenin nuclear translocation. Importantly, YAP and β-catenin co-localize in the nucleus while YAP interacts with β-catenin and regulates its target gene XBP1 leading to reduced NLRP3/caspase-1 activity after co-culture. Moreover, macrophage YAP or β-catenin deficiency augmented XBP1/NLRP3 while XBP1 deletion diminished NLRP3/caspase-1 activity. Increasing NLRP3 expression reduced M2 macrophage Arg1 but augmented M1 macrophage iNOS expression accompanied by increased IL-1β release. Conclusion: MSCs promote macrophage Hippo pathway, which in turn controls NLRP3 activation through a direct interaction between YAP and β-catenin and regulates XBP1-mediated NLRP3 activation leading to reprograming macrophage polarization towards an anti-inflammatory M2 phenotype. Moreover, YAP functions as a transcriptional co-activator of β-catenin in MSC-mediated immune regulation. Our findings provide a novel therapeutic target in MSC-mediated immunotherapy of liver sterile inflammatory injury.

Contact: Bibo Ke, MD, PhD, The Dumont-UCLA Transplant Center, Department of Surgery, David Geffen School of Medicine at UCLA, 77-120 CHS, 10833 Le Conte Ave, Los Angeles, CA 90095. Tel: (310) 825-7444; Fax: (310) 267-2367, bke@mednet.ucla.edu.

Author names in bold designate shared co-first authorship

Keywords

YAP; β-catenin; Macrophage polarization; Innate immunity; Liver inflammation

Multipotent mesenchymal stem cells (MSCs) have been shown a promising therapeutic potential for the tissue damage and inflammation owing to their unique immunoregulatory properties. Previous studies have shown that interactions between MSCs and inflammatory cells are crucial in MSC-mediated immune modulation and tissue repair (1). With the ability to regulate both the innate and adaptive immune systems, MSC-based therapy has been successfully applied in various immune-mediated diseases in humans (2). However, a number of phase III clinical trials of MSC immunotherapy were unable to meet the primary endpoints because of the low immunoregulatory efficacy of engrafted cells (3). Thus, exploring novel modulatory mechanisms that govern the immunosuppressive potential of MSC emerges as one of the key challenges of MSC therapy.

Hippo signaling pathway is an evolutionarily conserved pathway that regulates mammalian organ size by controlling cell proliferation, apoptosis and stem cell self-renewal (4). YAP, as a key downstream transcriptional coactivator of the Hippo signaling pathway, functions to negatively regulate the target gene activities (5). Indeed, YAP is modulated by its upstream kinases mammalian Ste20-like kinase (MST)1 and MST2. Phosphorylation of MST1/2 activates large tumor suppressor (LATS)1 and LATS2, which in turn phosphorylates YAP leading to the nuclear exclusion of YAP and, ultimately, their cytoplasmic degradation (5). However, unphosphorylated YAP enter the nucleus where they interact with a variety of transcription factors to regulate gene expression that promotes cell proliferation, differentiation, and survival (5). It was shown that YAP can control organ size, most notably in the liver (6). Increasing YAP expression contributed to the wound repair and tissue regeneration in inflammatory injury (7). Moreover, recent evidence has indicated that Hippo signaling regulates innate immunity through a YAP-mediated transcriptional mechanism (8). Activation of YAP inhibited immune response while YAP deficiency resulted in aggravated tissue inflammatory injury (9).

β-catenin, a canonical Wnt signaling pathway, is key for the cell proliferation, development, and tissue homeostasis (10). Activation of the canonical Wnt/β-catenin pathway promotes bone marrow-derived MSC differentiation and confers resistance to oxidative stress in tissue injury (11). We have previously demonstrated that myeloid β-catenin can regulate NLRP3-mediated innate immunity in liver IRI (12, 13). Activation of β-catenin regulates cell differentiation is associated with the Hippo-YAP pathway (14), YAP may physically interact with β-catenin to regulate tissue homeostasis and regeneration (15). Although several reports have shown that Hippo signaling can be integrated with other pathways to coordinately regulate biological processes (16), and MSCs can program macrophage plasticity and modulate inflammatory response by secreting PGE2 (17), it remains largely unknown as to whether and how the Hippo-YAP signaling may regulate NLRP3 activation and mediate the immunoregulatory function of MSCs in liver inflammatory injury.

In the present study, we have identified a novel functional role and regulatory mechanism of the Hippo signaling in MSC-mediated immune regulation. We demonstrate that MSCs

promote macrophage Hippo-YAP pathway and control NLRP3 activation through a direct interaction between YAP and β-catenin, which in turn regulates their target gene XBP1 leading to reprograming macrophage polarization from a pro-inflammatory M1 to an anti-inflammatory M2 phenotype in IR-triggered liver inflammation.

Experimental Procedures

Animals.

The floxed YAP ($YAP^{FL/FL}$) mice and the mice expressing the Cre recombinase under the control of the Lysozyme M (LysM) promoter were used to generate myeloid-specific YAP knockout ($YAP^{M\text{-}KO}$) mice (Supplementary Fig. 1). The β-$catenin^{M\text{-}KO}$ mice were generated as described (13). This study was performed in strict accordance with the recommendations in the *Guide for the Care and Use of Laboratory Animals* published by the NIH. The study protocols were approved by the Institutional Animal Care and Use Committee of University of California at Los Angeles. See Supplementary Materials.

Mouse liver IRI model and treatment.

We used a well-established mouse model of warm hepatic ischemia (90 min) followed by reperfusion (6 h), as described (12). Some animals were injected via tail vein with bone marrow-derived MSCs (1×10^6cells in PBS/mouse) or pre-labeled with 5-chloromethylfluorescein diacetate (CMFDA) green fluorescent dye (Invitrogen) 24h prior to ischemia. See Supplementary Materials.

Hepatocellular function assay.

Serum alanine aminotransferase (sALT) levels, an indicator of hepatocellular injury, were measured by IDEXX Laboratories (Westbrook, ME).

Histology and immunofluorescence staining.

Liver sections were stained with hematoxylin and eosin (H&E). The severity of IRI was graded using Suzuki's histological criteria (18). Liver macrophages and bone marrow-derived macrophages (BMMs) were detected using primary goat anti-mouse CD68, rabbit anti-mouse Arg1, and rabbit anti-mouse β-catenin or YAP mAbs for immunofluorescence staining. See Supplementary Materials.

Quantitative RT-PCR analysis.

Quantitative real-time PCR was performed as described (13). Primer sequences used for the amplification are shown in Supplementary Table 1. See Supplementary Materials.

Immunoblot analysis.

Protein was extracted from liver tissue or cell cultures as described (13). The nuclear and cytosolic fractions were prepared with NE-PER Nuclear and Cytoplasmic Extraction Reagents. Rabbit anti-mouse β-catenin, p-β-catenin, p-MST½, MST½, p-LATS1, LATS1, p-YAP, YAP, Arg1, iNOS, XBP1s, NLRP3, cleaved caspase-1, p-Akt, Akt, Lamin B, and β-actin Abs (Cell Signaling Technology) were used. See Supplementary Materials.

Immunoprecipitation analysis.

BMMs from co-culture were lysed in NP-40 lysis buffer. The lysates were incubated with β-catenin antibody or control IgG and protein A/G beads at 4 °C overnight. After immunoprecipitation, the immunocomplexes were analyzed by standard immunoblot procedures. See Supplementary Materials.

Isolation of hepatic Kupffer cells, BMMs and bone marrow-derived MSCs.

Primary liver macrophages (Kupffer cells) and BMMs were isolated, as described (13). Bone marrow-derived MSCs were isolated, as described (19). See Supplementary Materials.

In vitro transfection.

BMMs (1×10^6) were transfected with CRISPR/Cas9 XBP1 knockout (KO), CRISPR YAP activation, CRISPR NLRP3 activation or CRISPR control vector (Santa Cruz Biotechnology) by using Lipofectamine™ 3000 according to the manufacturer's instructions (Invitrogen). See Supplementary Materials.

Co-culture of macrophages and MSCs.

Macrophages (1×10^6) were cultured in a 6-well plate. After 24h, MSCs (2×10^5) in a transwell insert were placed into the 6-well plate that macrophages were initially seeded. Co-cultures were incubated for 24h with or without adding LPS (100 ng/ml). See Supplementary Materials.

ELISA assay.

ELISA kits were used to measure PGE2, TNF-α, IL-1β, IL-10, and TGF-β levels in murine serum and co-culture supernatants. See Supplementary Materials.

Luciferase assays.

BMMs were co-transfected with β-catenin-luciferase and CRISPR YAP activation vectors and the transcriptional activity was measured using a luciferase assay system according to the manufacturer's instructions (Promega, WI). See Supplementary Materials.

Caspase-1 enzymatic activity assay.

Caspase-1 enzymatic activity was determined by a colorimetric assay kit (R&D System), as described (20). See Supplementary Materials.

Chromatin immunoprecipitation (ChIP) and ChIP-sequencing (ChIP-seq).

The ChIP analysis was carried out using ChIP Assay Kit (ABcam) according to the manufacturer's instructions. The ChIP-DNA was amplified to generate library for sequencing with an Illumina HiSeq3000 (Illumina) at the Technology Center for Genomics & Bioinformatics (TCGB) at UCLA. See Supplementary Materials.

Statistical analysis.

Data are expressed as mean±SD and analyzed by Permutation *t*-test and Pearson correlation. Per comparison two-sided *p* values less than 0.05 were considered statistically significant.

Multiple group comparisons were made using one-way ANOVA followed by Bonferroni's post hoc test. When groups showed unequal variances, we applied Welch's ANOVA to make multiple group comparisons. All analyses were used by SAS/STAT software, version 9.4.

Results

Adoptive transfer of MSCs attenuates IR-induced liver injury and inhibits proinflammatory mediators.

We used a mouse model of hepatic warm ischemia (90 min) followed by reperfusion to test the effect of MSCs *in vivo*. As MSC migration and recruitment are crucial to the success of MSC-mediated immune regulation, we determined whether exogenous MSCs may respond to signals of cellular damage to the sites of injury after liver IR. To track the distribution of MSCs in ischemic livers, MSCs were labeled with 5-CMFDA and adoptively transferred into WT mice. Indeed, increased number of MSCs (green) were recruited to the injured livers compared to the sham controls at 6h of reperfusion (Figure 1A). The hepatocellular function as measured by sALT levels (IU/L) was significantly improved after adoptive transfer of MSCs in mice compared to untreated controls (Figure 1B, 8,861±2,507.9 vs. 18,366±4,386.8, $p<0.01$). These functional data are correlated with Suzuki's histological grading of IR-mediated liver damage (Figure 1C). Unlike in controls which showed moderate or severe sinusoidal congestion, cytoplasmic vacuolization, and hepatocellular necrosis (Suzuki score=3.93±0.38), livers from MSC-treated mice exhibited well-preserved hepatic architecture, with minimal sinusoidal congestion and without edema, vacuolization or necrosis (Suzuki score=1.90±0.10, $p<0.01$). Consistent with the histopathological and hepatocellular function data, MSC treatment in mice significantly reduced the expression of pro-inflammatory TNF-α, IL-1β but augmented IL-10 and TGF-β compared to untreated controls (Figure 1D).

MSCs regulate Hippo signaling and β-catenin activation and control macrophage polarization in IR-stressed livers.

We then analyzed whether MSCs may influence the Hippo signaling and β-catenin activation in IR-induced liver injury. By 6h of reperfusion after 90min of ischemia, IR stress increased phosphorylation of MST½ (p-MST½) and LATS1 (p-LAST1) in ischemic livers. However, MSC treatment reduced p-MST½, p-LATS1, and p-YAP but augmented nuclear YAP expression after liver IRI (Figure 2A). Unlike in untreated controls, increased p-Akt, p-β-catenin at Ser552, and β-catenin were observed in MSC-treated livers (Figure 2A). The serum PGE2 production was significantly increased after MSC treatment (Figure 2B). Interestingly, using double immunofluorescence staining, we found that administration of MSCs increased M2 macrophage arginase1 (Arg1) expression (Figure. 2C), which resulted in reduced serum TNF-α and IL-1β but increased IL-10 and TGF-β production compared to the untreated controls (Figure. 2D). To determine whether MSCs specifically influence the Hippo-YAP pathway and β-catenin activation in liver macrophages, we isolated hepatic Kupffer cells from ischemic livers in WT mice. Indeed, MSC treatment augmented nuclear YAP and β-catenin expression (Figure 2E), which was accompanied by increased Arg1 and reduced iNOS expression (Figure 2F) in hepatic Kupffer cells.

Myeloid YAP deficiency in MSC-treated livers aggravates IR-induced hepatocellular damage and promotes NLRP3 inflammasome-driven inflammatory response.

As increased nuclear YAP expression was found in hepatic Kupffer cells after MSC treatment, we next determined whether YAP may play a role in the regulation of NLRP3-driven inflammatory response in IR-stressed livers after MSC intervention. The myeloid-specific YAP knockout ($YAP^{M\text{-}KO}$) and $YAP^{FL/FL}$ mice were treated with MSCs and subjected to liver IR. We isolated both hepatocytes and liver macrophages (Kupffer cells) from these ischemic livers. Indeed, $YAP^{M\text{-}KO}$ did not change hepatocyte YAP expression. However, the YAP expression was lacking in liver macrophages from the $YAP^{M\text{-}KO}$ mice but not from the $YAP^{FL/FL}$ mice (Figure 3A). Unlike livers in the $YAP^{FL/FL}$ mice, which showed mild to moderate edema without necrosis (Figure 3B, score=1.30±0.28) after MSC treatment, livers in the $YAP^{M\text{-}KO}$ mice revealed significant edema, severe sinusoidal congestion/cytoplasmic vacuolization, and extensive (30–50%) necrosis (Figure 3B, score=2.43±0.31, $p<0.05$). Consistent with this data, the sALT levels were significantly increased in the $YAP^{M\text{-}KO}$ mice even with concomitant MSC treatment, compared to the MSC-treated $YAP^{FL/FL}$ mice (Figure 3C, 7367±929.8 vs. 3367±564.2, $p<0.05$). Moreover, increased proinflammatory TNF-α and IL-1β and decreased anti-inflammatory IL-10 and TGF-β expression profile was observed in the $YAP^{M\text{-}KO}$ but not the $YAP^{FL/FL}$ livers after MSC treatment (Figure 3D). Strikingly, $YAP^{M\text{-}KO}$ augmented NLRP3 and cleaved caspase-1 protein expression (Figure 3E) with increased serum IL-1β release (Figure 3F), compared to the MSC-treated $YAP^{FL/FL}$ mice.

Disruption of myeloid β-catenin in MSC-treated livers activates NLRP3 and diminishes M2 macrophage polarization in IR-stressed livers.

As MSCs promoted Akt and β-catenin phosphorylation at Ser552, which resulted in translocation of β-catenin into nucleus (21), we then determined whether β-catenin may modulate NLRP3 function and macrophage differentiation in MSC-mediated immune regulation. The $\beta\text{-catenin}^{M\text{-}KO}$ and $\beta\text{-catenin}^{FL/FL}$ mice were treated with MSCs and subjected to liver IR. We found that the $\beta\text{-catenin}^{M\text{-}KO}$ aggravated IR-induced liver damage after MSC treatment as evidenced by the increased Suzuki's histological score (Figure 4A, score= 2.87±0.25 vs. 1.80±0.20, $p<0.05$) and sALT levels (Figure 4B, 7,422±1,422.3 vs. 4,472±1,132.3, $p<0.05$) compared to the MSC-treated $\beta\text{-catenin}^{FL/FL}$ controls. Consistent with the histopathological and hepatocellular function data, the mRNA levels coding for TNF-α and IL-1β were significantly increased in the $\beta\text{-catenin}^{M\text{-}KO}$ whereas IL-10 and TGF-β levels were reduced in the $\beta\text{-catenin}^{M\text{-}KO}$ livers compared to the $\beta\text{-catenin}^{FL/FL}$ controls (Figure 4C). Moreover, immunoblot analysis revealed that increased NLRP3 and cleaved caspase-1 protein levels (Figure 4D) and IL-1β release (Figure 4E) were found in the $\beta\text{-catenin}^{M\text{-}KO}$ but not in the $\beta\text{-catenin}^{FL/FL}$ livers after MSC treatment. The $\beta\text{-catenin}^{M\text{-}KO}$ diminished macrophage Arg1 expression in MSC-treated livers compared to the $\beta\text{-catenin}^{FL/FL}$ controls (Figure 4F).

YAP interacts with β-catenin and regulates its transcription activity in MSC-mediated immune regulation.

Having demonstrated the importance of both the Hippo-YAP pathway and β-catenin in the modulation of NLRP3 function *in vivo* after MSC intervention, we next tested whether there is crosstalk between the Hippo-YAP pathway and β-catenin in MSC-mediated immune regulation. Using a Transwell system, BMMs were co-cultured with MSCs followed by LPS stimulation. Immunofluorescent staining revealed increased nuclear YAP (Figure 5A) and β-catenin (Figure 5B) expression in macrophages after co-culture with MSCs. This was further confirmed by Western blots, which showed increased macrophage nuclear YAP and β-catenin protein expression after co-culture (Figure 5C). Interestingly, both YAP and β-catenin were co-localized in the nucleus (Figure 5D). Moreover, co-immunoprecipitation assays revealed that YAP can bind to endogenous β-catenin in macrophages after co-culture (Figure 5E). YAP stimulated β-catenin transcriptional activity in a dose-dependent manner, as evidenced by consistently increased β-catenin-luciferase reporter gene (Figure 5F).

The YAP-β-catenin signaling targets XBP1 and inhibits NLRP3-driven inflammatory response in MSC-mediated immune regulation.

To explore the potential mechanism of the YAP-β-catenin signaling in the modulation of NLRP3 activation in MSC-mediated immune regulation, we performed β-catenin ChIP coupled to massively parallel sequencing (ChIP-Seq) (Figure 6A). Clearly, β-catenin ChIP-seq peaks were identified within the Xbp1 gene. One was located in the promoter region, and others were located within the intron or exon (Figure 6B). To validate the ChIP-seq peak located in the Xbp1 promoter region, ChIP-PCR was performed using β-catenin and YAP antibodies in MSC-treated BMMs. After ChIP with YAP or β-catenin antibody, primer was designed to detect the β-catenin/TCF DNA-binding site in Xbp1 promoter by PCR analysis. To confirm that YAP is co-localized with β-catenin on the promoter of Xbp1, sequential ChIPs were performed. The first ChIP was performed with β-catenin antibody and the second ChIP was carried out with either YAP or β-catenin antibody using the chromatin eluted from the first ChIP. Following the second ChIP, both YAP and β-catenin were still bound to the β-catenin/TCF-binding motif in the β-catenin-chromatin complex (Figure 6C), confirming that YAP and β-catenin are present at the same promoter region of Xbp1. Hence, Xbp1 is a target gene regulated by the YAP-β-catenin complex. Moreover, MSCs reduced macrophage p-MST½, p-LATS1, and p-YAP but augmented nuclear YAP levels (Figure 6D). However, increased macrophage Akt and β-catenin phosphorylation and nuclear β-catenin expression (Figure 6E) accompanied by diminished XBP1s, NLRP3, and cleaved caspase-1 expression (Figure 6F) were observed after co-culture with MSCs. This result was confirmed by caspase-1 activity assay, which showed that MSCs significantly reduced macrophage caspase-1 activity in co-cultures (Figure 6G).

YAP-β-catenin signaling is essential for the modulation of XBP1 and reprograms NLRP3-dependent macrophage polarization in MSC-mediated immune regulation.

To elucidate the mechanistic role of the Hippo-YAP pathway and β-catenin signaling in the control of XBP1/NLRP3 activation in MSC-mediated immune regulation, BMMs were isolated from the β-catenin$^{FL/FL}$, β-catenin$^{M\text{-}KO}$, YAP$^{FL/FL}$, and YAP$^{M\text{-}KO}$ mice. β-catenin

or YAP deficiency augmented XBP1s accompanied by increased NLRP3 and cleaved caspase-1 expression in macrophages after co-culture with MSCs (Figure 7A and 7B). Overexpression of YAP by transfecting CRISPR-mediated YAP activation diminished XBP1s expression in β-catenin-proficient macrophages (Figure 7C). However, the expression of XBP1s was not significantly changed in β-catenin-deficient macrophages after transfection of CRISPR-mediated YAP activation (Figure 7C), suggesting that the YAP-β-catenin interaction is crucial for the regulation of XBP1 activation. Indeed, macrophage XBP1 is activated by IRE1α, a stress sensor, which signals innate immunity during inflammatory response (22). Moreover, activation macrophage IRE1α signaling is required for NLRP3 activation (23). These reports imply that XBP1 may play a role in the regulation of NLRP3 function. To dissect the role of the β-catenin/XBP1 axis on NLRP3 activation in macrophages, BMMs from β-catenin$^{M\text{-}KO}$ mice were transfected with a CRISPR/Cas9 XBP1 knockout vector and then co-cultured with MSCs. Strikingly, XBP1 deficiency resulted in decreased NLRP3 and cleaved caspase-1 expression (Figure 7D). To determine whether NLRP3 is associated with macrophage polarization after co-culture with MSCs, we transfected BMMs with CRISPR-mediated NLRP3 activation vector or control vector followed by LPS stimulation. Clearly, compared with the control vector, transfection of CRISPR-mediated NLRP3 activation vector in BMMs markedly increased NLRP3, cleaved caspase-1, and iNOS but depressed Arg1 expression (Figure 7E) accompanied by augmented IL-1β release (Figure 7F) after co-culture with MSCs. Furthermore, reduced Arg1 positive macrophages were observed in NLRP3-transfected groups compared to the control vector-transfected cells (Figure 7G). Consistent with these results, transfection of CRISPR-mediated NLRP3 activation vector in BMMs increased TNF-α and IL-1β but reduced IL-10 and TGF-β mRNA levels compared to the control vector-transfected cells (Figure 7H).

Discussion

This study is the first to document the key role of Hippo signaling in controlling NLRP3-driven innate immune responses and mediating immunoregulatory properties of MSCs in a liver sterile inflammatory injury. We demonstrate that: i) adoptive transfer of MSCs alleviates IR-induced liver inflammation by modulating crosstalk between macrophage Hippo signaling downstream effector YAP and β-catenin activation; ii) YAP is co-localized and interacts with β-catenin, which in turn regulates their target gene XBP1 leading to reduced NLRP3/caspase-1 activity; iii) YAP is crucial to mediate β-catenin transcriptional activity and reprograms NLRP3-dependent macrophage polarization in MSC-mediated immune regulation. Our results highlight the importance of macrophage YAP-β-catenin complex as a key regulator of the NLRP3 function in MSC-mediated immune regulation during liver inflammatory injury.

Although various studies have demonstrated that MSCs exert immunosuppressive effects and MSC-based therapy has been shown a therapeutic potential in various human diseases (24), it is the greatest challenge to overcome the low immunosuppressive efficacy of engrafted cells. Understanding novel immuoregulatory mechanisms of MSCs is crucial to improve immunosuppressive properties of MSCs for the next generation stem cell therapeutics. In our current study, we revealed that adoptive transfer of MSCs reduced IR-induced hepatocellular damage and ameliorated hepatic function. Interestingly, MSC

treatment promoted the Hippo pathway downstream effector YAP and activated β-catenin signaling, accompanied by augmented M2 macrophage phenotype and anti-inflammatory program in IR-stressed livers. These results imply that the Hippo pathway and β-catenin signaling play pivotal roles and modulation of their signaling pathways may provide a possible targeting strategy in MSC-mediated immune regulation in IR-stressed liver.

As β-catenin has been indicated to regulate immune response in inflammatory diseases (25), MSC-mediated β-catenin signaling could act as a native regulator for NLRP3 activation in macrophages. We found that myeloid β-catenin deficiency exacerbated IR-induced liver damage even with concomitant MSC treatment. Disruption of β-catenin activated NLRP3 and caspase-1, a key mediator in processing proinflammatory cytokine IL-1β from an inactive precursor to an active, secreted molecule to trigger innate immune response (26). Notably, myeloid β-catenin-deficiency reduced M2 while increasing M1 macrophage phenotype accompanied by decreased IL-10/TGF-β and increased TNF-α/IL-1β expression in MSC-treated IR-livers, suggesting the importance of myeloid β-catenin in the modulation of macrophage polarization. Indeed, the β-catenin signaling has shown multiple regulatory functions during inflammatory response. Activation of β-catenin enhances MSC migration ability to the injury sites for the tissue repair (11, 27). Consistent with our previous reports that β-catenin regulated liver inflammatory response by controlling TLR4 signaling to program innate and adaptive immunity (12), our present results imply that myeloid β-catenin is essential for the modulation of NLRP3 function in MSC-mediated immune regulation.

One striking finding was that MSCs regulated macrophage Hippo pathway, especially increased YAP nuclear translocation to control liver inflammation in IR-stressed livers. Indeed, YAP has been shown a major regulator of tissue growth and development (28). Transgene-mediated YAP induction increases cell proliferation (29) while activation of YAP reprograms cell activity and facilitates efficient tissue repair during inflammatory injury (7). Although the emerging roles of Hippo signaling in inflammation is based on different cell context and microenvironment (30), YAP displays a distinct ability to regenerate and repair following partial liver damage (31). We found that IR stress promoted Hippo core kinase signaling cascade (MST½-LATS1) and phosphorylated YAP to accomplish its cytoplasmic sequestration, which in turn triggered liver inflammation, evidenced by increased proinflammatory cytokine profile. However, MSC administration restricted the kinases MST½ and LATS1 phosphorylation and increased YAP nuclear translocation, leading to augmented M2 macrophage phenotype and anti-inflammatory mediators. Moreover, although the decreased inflammation was observed in MSC-treated $YAP^{FL/FL}$ mice, YAP deficiency resulted in enhanced NLRP3/caspase-1 activity and exacerbated liver inflammatory injury in $YAP^{M\text{-}KO}$ mice after MSC treatment. Our findings document the ability of the Hippo-YAP pathway to control NLRP3-driven inflammation in IR-stressed liver.

As both YAP and β-catenin signaling play important roles in the regulation of NLRP3 function in liver IRI after MSC treatment, the question arises as to what other mechanisms may confer YAP and β-catenin with their ability to selectively affect NLRP3 activation in MSC-mediated immune regulation. We found that IR stress increased PGE2 section from MSCs and activated macrophage Akt, which phosphorylated β-catenin at Ser552 resulted in

translocation of β-catenin into nucleus after MSC treatment. This is consistent with previous report that β-catenin activity is dependent on Akt phosphorylation (21). However, IR stress induced phosphorylation of MST½ and LATS1 while MSC treatment reduced MST½ and LATS1 phosphorylation leading to increased YAP nuclear translocation in ischemic livers, suggesting that MSC-mediated immune regulation may be involved in both YAP and β-catenin activity. Although β-catenin activity is regulated through multiple mechanisms, we have shown previously that activation of β-catenin modulates innate immune response by nuclear translocation of β-catenin in macrophages and alleviates IR-induced liver injury (12). Thus, we speculate that nuclear localization of endogenous YAP and β-catenin is essential for transcriptional activity in MSC-mediated immune regulation during liver IRI. This was confirmed by our *in vitro* MSC/macrophage co-culture system. Indeed, we found that macrophage YAP and β-catenin co-localized in the nucleus and YAP mediated β-catenin transcriptional activity. The ChIP and ChIP sequencing data further revealed that YAP was co-localized with β-catenin on the promoter of Xbp1, suggesting that Xbp1 is a target gene regulated by the YAP and β-catenin complex while YAP acts as a transcriptional co-activator of β-catenin. Moreover, β-catenin deficiency promoted XBP1 and NLRP3/caspase-1 activation in macrophages after co-culture with MSCs whereas XBP1 deletion augmented NLRP3/caspase-1 activity. Consistent with our previous findings that activation of XBP1 enhanced NLRP3-driven inflammatory response in liver IRI (13), XBP1 is essential for the activation of NLRP3 in response to inflammatory stimuli. Taken together, these results reveal a novel crosstalk between macrophage YAP and β-catenin signaling in the modulation of NLRP3 function. YAP interacts with β-catenin, which in turn regulates its target gene XBP1 leading to reduced NLRP3/caspase-1 activity. Hence, our current findings demonstrated a fundamental role of Hippo signaling in regulating NLRP3-mediated innate immune response in MSC-mediated immune regulation.

Another important implication of our results is that the YAP-β-catenin interaction is key to shift macrophage polarization towards M2 macrophage phenotype in MSC-mediated immune regulation. We have shown that myeloid YAP or β-catenin deficiency reduced M2 macrophage Arg1 expression while increasing proinflammatory cytokine genes in MSC-treated livers in response to IR stress. Moreover, macrophage depletion by clodronate liposome treatment in ischemic livers dampened MSC-mediated immune regulation (Supplementary Fig. 2). It is less clear how the YAP-β-catenin complex regulates macrophage polarization from a proinflammatory M1 to an anti-inflammatory M2 phenotype in IR-triggered liver inflammation after MSC intervention. It is known that YAP or β-catenin deficiency enhances innate immune response (13, 32) while activation of YAP or β-catenin orchestrates immunosuppressive response following tissue injury (9, 25). In line with these findings, we found that MSC promoted YAP and β-catenin activation, which in turn inhibited NLRP3 expression whereas disruption of YAP or β-catenin enhanced XBP1-mediated NLRP3/caspase-1 activity. Importantly, increasing NLRP3 expression inhibited M2 macrophage Arg1 but enhanced M1 macrophage iNOS expression with increased IL-1β release after co-culture with MSCs. Thus, NLRP3 is key to balance M1/M2 macrophage polarization in YAP-β-catenin-mediated regulation. Our results revealed a crucial role of the YAP-β-catenin complex in controlling a dynamic crosstalk with the NLRP3 in MSC-mediated immune regulation.

It is worth noting that other regulatory molecules and pathways may also relate to NLRP3 function in sterile inflammation. It was reported that miR-223 is required for the regulation of NLRP3-driven inflammation in intestine and lung (33, 34). Under ischemic or hypoxic conditions, purinergic receptors play important roles in triggering inflammatory response and tissue injury (35, 36). The purinergic receptor signaling was crucial for the ATP-mediated NLRP3 activation in allograft rejection (36). Interestingly, the purinergic receptors induced cell proliferation and migration in injured tissues by regulating YAP activation (37), suggesting that there is a crosstalk between purinergic receptors and the Hippo-YAP pathway. Moreover, the hypoxia-inducible factors regulated their target genes leading to resistance to ischemia and controlling excessive inflammation (38, 39), which may interact with YAP under hypoxic conditions (40). These reports suggest that Hippo pathway-mediated immune regulation may involve in multiple signaling pathways during sterile inflammatory injury.

Indeed, liver IRI represents one of the most understudied yet critical problems as it often leads to primary graft non-function or failure in transplant recipients. However, during surgical procedure, patients may be also threatened by perioperative other type of organ injuries (41). Thus, it is crucial to develop novel therapeutic approaches for the prevention or treatment of perioperative organ injury (41). Our current study provides new mechanistic insights into liver IRI and might also provide novel therapeutic potentials for the transplant inflammatory injury and other type of organ injuries in MSC-mediated immune regulation.

Figure 8 depicts putative molecular mechanisms by which Hippo signaling may regulate NLRP3 activation in MSC-mediated immune regulation. IR stress increases MSC-mediated PGE2 secretion, which in turn activates macrophage Akt and phosphorylates β-catenin at Ser552 leading to translocation of β-catenin into nucleus. Notably, MSCs regulate macrophage Hippo-YAP pathway by depressing MST½ and LATS1 phosphorylation, and increasing YAP translocation from cytoplasm to nucleus where YAP co-localizes and interacts with nuclear β-catenin, which in turn regulates their target gene XBP1 leading to reduced NLRP3/caspase-1 activity and IL-1β release, and augmented M2 macrophage phenotype in IR-triggered liver inflammation.

In conclusion, we identify a previously unrecognized roles of Hippo signaling in controlling NLRP3 activation in MSC-mediated immune regulation. Our findings demonstrate that YAP is a novel coactivator of β-catenin and the YAP-β-catenin interaction is crucial for the inhibition of XBP1-mediated NLRP3 activation and reprograms macrophage differentiation during liver sterile inflammatory injury. Indeed, as a key regulator of NLRP3-driven inflammation in liver IRI, the Hippo signaling downstream effector YAP is a therapeutic target. We may develop novel therapeutic strategies to treat transplant recipients using genetically modified MSC approaches or pharmacological interventions targeting YAP in the donor or in the graft before implantation or reperfusion.

Supplementary Material

Refer to Web version on PubMed Central for supplementary material.

Acknowledgments

Supported by: NIH Grants R01AI139552, R21AI112722, R21AI115133 (B.KE), P01AI120944, R01DK062357, R01DK102110, R01DK107533 (J.W.K-W), and The Dumont Research Foundation.

Abbreviations:

Arg1	arginase1
BMMs	bone marrow-derived macrophages
CRISPR	clustered regularly interspaced short palindromic repeats
Cas9	CRISPR associated protein 9
ChIP	Chromatin immunoprecipitation
ChIP-seq	ChIP-sequencing
CMFDA	5-chloromethylfluorescein diacetate
iNOS	inducible nitric oxide synthase
IRI	ischemia/reperfusion injury
LATS	large tumor suppressor
LPS	lipopolysaccharide
MSCs	mesenchymal stem cells
MST	mammalian Ste20-like kinase
NLRP3	NLR family pyrin domain containing 3
PGE2	prostaglandin E2
siRNA	small interfering RNA
sALT	serum alanine aminotransferase
YAP	yes-associated protein

References

1. Dimarino AM, Caplan AI, Bonfield TL. Mesenchymal stem cells in tissue repair. Front Immunol 2013;4:201. [PubMed: 24027567]
2. Wang LT, Ting CH, Yen ML, Liu KJ, Sytwu HK, Wu KK, Yen BL. Human mesenchymal stem cells (MSCs) for treatment towards immune- and inflammation-mediated diseases: review of current clinical trials. J Biomed Sci 2016;23:76. [PubMed: 27809910]
3. Karp JM, Leng Teo GS. Mesenchymal stem cell homing: the devil is in the details. Cell Stem Cell 2009;4:206–216. [PubMed: 19265660]
4. Zhao B, Tumaneng K, Guan KL. The Hippo pathway in organ size control, tissue regeneration and stem cell self-renewal. Nat Cell Biol 2011;13:877–883. [PubMed: 21808241]
5. Saucedo LJ, Edgar BA. Filling out the Hippo pathway. Nat Rev Mol Cell Biol 2007;8:613–621. [PubMed: 17622252]

6. Yu FX, Zhao B, Guan KL. Hippo Pathway in Organ Size Control, Tissue Homeostasis, and Cancer. Cell 2015;163:811–828. [PubMed: 26544935]
7. Yui S, Azzolin L, Maimets M, Pedersen MT, Fordham RP, Hansen SL, Larsen HL, et al. YAP/TAZ-Dependent Reprogramming of Colonic Epithelium Links ECM Remodeling to Tissue Regeneration. Cell Stem Cell 2018;22:35–49 e37. [PubMed: 29249464]
8. Liu B, Zheng Y, Yin F, Yu J, Silverman N, Pan D. Toll Receptor-Mediated Hippo Signaling Controls Innate Immunity in Drosophila. Cell 2016;164:406–419. [PubMed: 26824654]
9. Ramjee V, Li D, Manderfield LJ, Liu F, Engleka KA, Aghajanian H, Rodell CB, et al. Epicardial YAP/TAZ orchestrate an immunosuppressive response following myocardial infarction. J Clin Invest 2017;127:899–911. [PubMed: 28165342]
10. Logan CY, Nusse R. The Wnt signaling pathway in development and disease. Annu Rev Cell Dev Biol 2004;20:781–810. [PubMed: 15473860]
11. Cai SX, Liu AR, Chen S, He HL, Chen QH, Xu JY, Pan C, et al. Activation of Wnt/beta-catenin signalling promotes mesenchymal stem cells to repair injured alveolar epithelium induced by lipopolysaccharide in mice. Stem Cell Res Ther 2015;6:65. [PubMed: 25889393]
12. Ke B, Shen XD, Kamo N, Ji H, Yue S, Gao F, Busuttil RW, et al. beta-catenin regulates innate and adaptive immunity in mouse liver ischemia-reperfusion injury. Hepatology 2013;57:1203–1214. [PubMed: 23081841]
13. Yue S, Zhu J, Zhang M, Li C, Zhou X, Zhou M, Ke M, et al. The myeloid heat shock transcription factor 1/beta-catenin axis regulates NLR family, pyrin domain-containing 3 inflammasome activation in mouse liver ischemia/reperfusion injury. Hepatology 2016;64:1683–1698. [PubMed: 27474884]
14. Huraskin D, Eiber N, Reichel M, Zidek LM, Kravic B, Bernkopf D, von Maltzahn J, et al. Wnt/beta-catenin signaling via Axin2 is required for myogenesis and, together with YAP/Taz and Tead1, active in IIa/IIx muscle fibers. Development 2016;143:3128–3142. [PubMed: 27578179]
15. Azzolin L, Panciera T, Soligo S, Enzo E, Bicciato S, Dupont S, Bresolin S, et al. YAP/TAZ incorporation in the beta-catenin destruction complex orchestrates the Wnt response. Cell 2014;158:157–170. [PubMed: 24976009]
16. Irvine KD. Integration of intercellular signaling through the Hippo pathway. Semin Cell Dev Biol 2012;23:812–817. [PubMed: 22554983]
17. Nemeth K, Leelahavanichkul A, Yuen PS, Mayer B, Parmelee A, Doi K, Robey PG, et al. Bone marrow stromal cells attenuate sepsis via prostaglandin E(2)-dependent reprogramming of host macrophages to increase their interleukin-10 production. Nat Med 2009;15:42–49. [PubMed: 19098906]
18. Suzuki S, Toledo-Pereyra LH, Rodriguez FJ, Cejalvo D. Neutrophil infiltration as an important factor in liver ischemia and reperfusion injury. Modulating effects of FK506 and cyclosporine. Transplantation 1993;55:1265–1272. [PubMed: 7685932]
19. Li C, Kong Y, Wang H, Wang S, Yu H, Liu X, Yang L, et al. Homing of bone marrow mesenchymal stem cells mediated by sphingosine 1-phosphate contributes to liver fibrosis. J Hepatol 2009;50:1174–1183. [PubMed: 19398237]
20. Kamo N, Ke B, Ghaffari AA, Shen XD, Busuttil RW, Cheng G, Kupiec-Weglinski JW. ASC/caspase-1/IL-1beta signaling triggers inflammatory responses by promoting HMGB1 induction in liver ischemia/reperfusion injury. Hepatology 2013;58:351–362. [PubMed: 23408710]
21. Fang D, Hawke D, Zheng Y, Xia Y, Meisenhelder J, Nika H, Mills GB, et al. Phosphorylation of beta-catenin by AKT promotes beta-catenin transcriptional activity. J Biol Chem 2007;282:11221–11229. [PubMed: 17287208]
22. Martinon F, Chen X, Lee AH, Glimcher LH. TLR activation of the transcription factor XBP1 regulates innate immune responses in macrophages. Nat Immunol 2010;11:411–418. [PubMed: 20351694]
23. Robblee MM, Kim CC, Porter Abate J, Valdearcos M, Sandlund KL, Shenoy MK, Volmer R, et al. Saturated Fatty Acids Engage an IRE1alpha-Dependent Pathway to Activate the NLRP3 Inflammasome in Myeloid Cells. Cell Rep 2016;14:2611–2623. [PubMed: 26971994]
24. Trounson A, McDonald C. Stem Cell Therapies in Clinical Trials: Progress and Challenges. Cell Stem Cell 2015;17:11–22. [PubMed: 26140604]

25. Manicassamy S, Reizis B, Ravindran R, Nakaya H, Salazar-Gonzalez RM, Wang YC, Pulendran B. Activation of beta-catenin in dendritic cells regulates immunity versus tolerance in the intestine. Science 2010;329:849–853. [PubMed: 20705860]
26. Schroder K, Tschopp J. The inflammasomes. Cell 2010;140:821–832. [PubMed: 20303873]
27. Li X, He L, Yue Q, Lu J, Kang N, Xu X, Wang H, et al. MiR-9–5p promotes MSC migration by activating beta-catenin signaling pathway. Am J Physiol Cell Physiol 2017;313:C80–C93. [PubMed: 28424168]
28. Varelas X The Hippo pathway effectors TAZ and YAP in development, homeostasis and disease. Development 2014;141:1614–1626. [PubMed: 24715453]
29. Dong J, Feldmann G, Huang J, Wu S, Zhang N, Comerford SA, Gayyed MF, et al. Elucidation of a universal size-control mechanism in Drosophila and mammals. Cell 2007;130:1120–1133. [PubMed: 17889654]
30. Zhou Y, Huang T, Zhang J, Cheng ASL, Yu J, Kang W, To KF. Emerging roles of Hippo signaling in inflammation and YAP-driven tumor immunity. Cancer Lett 2018;426:73–79. [PubMed: 29654891]
31. Lu L, Finegold MJ, Johnson RL. Hippo pathway coactivators Yap and Taz are required to coordinate mammalian liver regeneration. Exp Mol Med 2018;50:e423. [PubMed: 29303509]
32. Wang S, Xie F, Chu F, Zhang Z, Yang B, Dai T, Gao L, et al. YAP antagonizes innate antiviral immunity and is targeted for lysosomal degradation through IKKvarepsilon-mediated phosphorylation. Nat Immunol 2017;18:733–743. [PubMed: 28481329]
33. Neudecker V, Haneklaus M, Jensen O, Khailova L, Masterson JC, Tye H, Biette K, et al. Myeloid-derived miR-223 regulates intestinal inflammation via repression of the NLRP3 inflammasome. J Exp Med 2017;214:1737–1752. [PubMed: 28487310]
34. Neudecker V, Brodsky KS, Clambey ET, Schmidt EP, Packard TA, Davenport B, Standiford TJ, et al. Neutrophil transfer of miR-223 to lung epithelial cells dampens acute lung injury in mice. Sci Transl Med 2017;9.
35. Riegel AK, Faigle M, Zug S, Rosenberger P, Robaye B, Boeynaems JM, Idzko M, et al. Selective induction of endothelial P2Y6 nucleotide receptor promotes vascular inflammation. Blood 2011;117:2548–2555. [PubMed: 21173118]
36. Idzko M, Ferrari D, Riegel AK, Eltzschig HK. Extracellular nucleotide and nucleoside signaling in vascular and blood disease. Blood 2014;124:1029–1037. [PubMed: 25001468]
37. Khalafalla FG, Greene S, Khan H, Ilves K, Monsanto MM, Alvarez R Jr., Chavarria M, et al. P2Y2 Nucleotide Receptor Prompts Human Cardiac Progenitor Cell Activation by Modulating Hippo Signaling. Circ Res 2017;121:1224–1236. [PubMed: 28923792]
38. Koeppen M, Lee JW, Seo SW, Brodsky KS, Kreth S, Yang IV, Buttrick PM, et al. Hypoxia-inducible factor 2-alpha-dependent induction of amphiregulin dampens myocardial ischemia-reperfusion injury. Nat Commun 2018;9:816. [PubMed: 29483579]
39. Bartels K, Grenz A, Eltzschig HK. Hypoxia and inflammation are two sides of the same coin. Proc Natl Acad Sci U S A 2013;110:18351–18352. [PubMed: 24187149]
40. Ma X, Zhang H, Xue X, Shah YM. Hypoxia-inducible factor 2alpha (HIF-2alpha) promotes colon cancer growth by potentiating Yes-associated protein 1 (YAP1) activity. J Biol Chem 2017;292:17046–17056. [PubMed: 28848049]
41. Bartels K, Karhausen J, Clambey ET, Grenz A, Eltzschig HK. Perioperative organ injury. Anesthesiology 2013;119:1474–1489. [PubMed: 24126264]

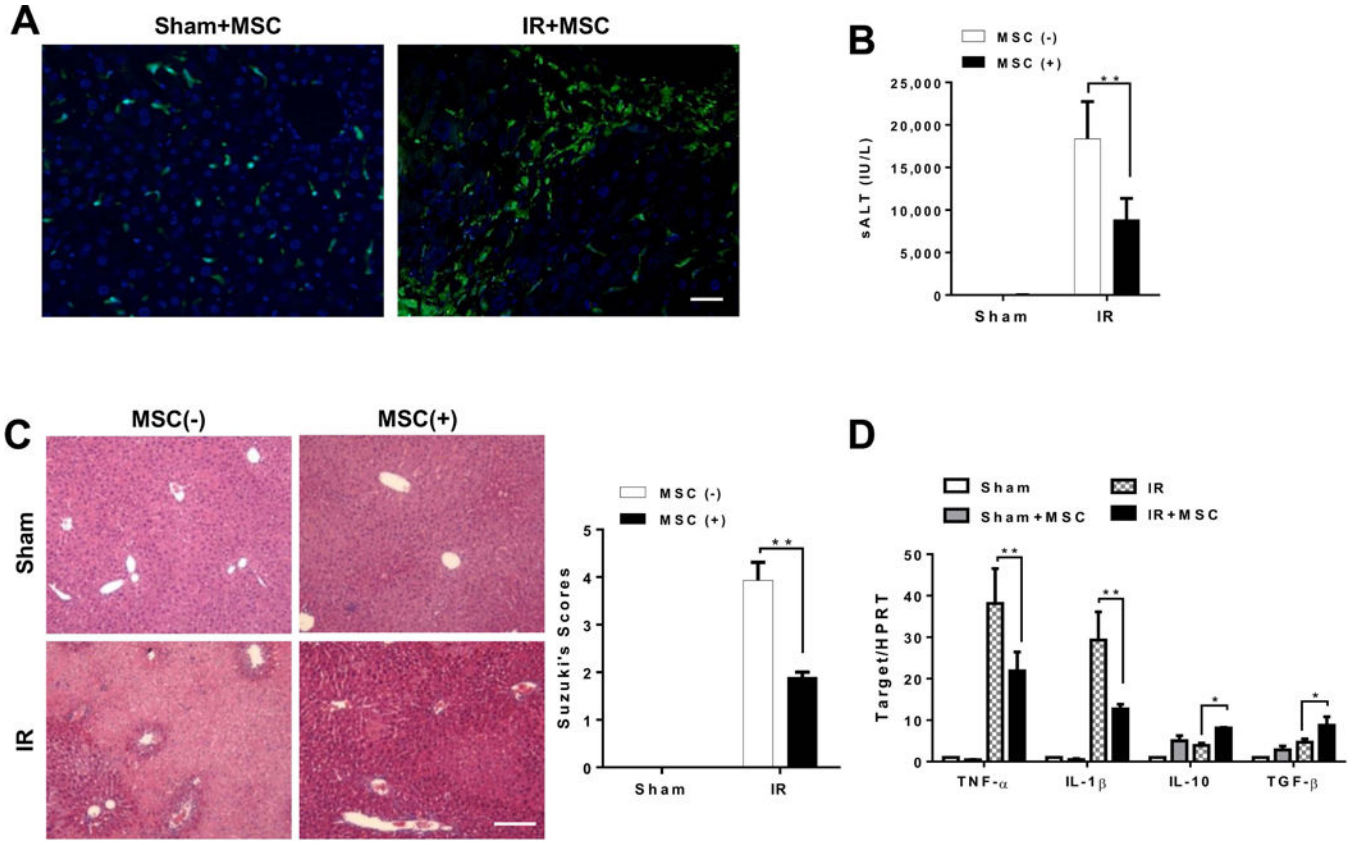

Figure 1. Adoptive transfer of MSCs attenuates IR-induced liver injury and inhibits proinflammatory mediator program.

Mice were subjected to 90min of partial liver warm ischemia, followed by 6h of reperfusion. Some animals were injected via tail vein with MSCs (1×10^6) 24h prior to ischemia insult. (A) MSCs were labeled with 5-CMFDA to track the distribution of MSCs in ischemic livers. Representative immunofluorescence staining for the MSCs labeled with 5-CMFDA (green) localized in IR-stressed livers after MSC treatment (n=3–4 mice/group). DAPI was used to visualize nuclei (blue). Scale bars, 20μm. (B) Hepatocellular function was evaluated by sALT levels (IU/L) (n=4–6 samples/group). (C) Representative histological staining (H&E) of ischemic liver tissue (n=4–6 mice/group) and Suzuki's histological score. Scale bars, 100μm. (D) qRT-PCR-assisted detection of TNF-α, IL-1β, IL-10, and TGF-β in ischemic livers (n=3–4 samples/group). Data were normalized to HPRT gene expression. All data represent the mean±SD. *p<0.05, **p<0.01.

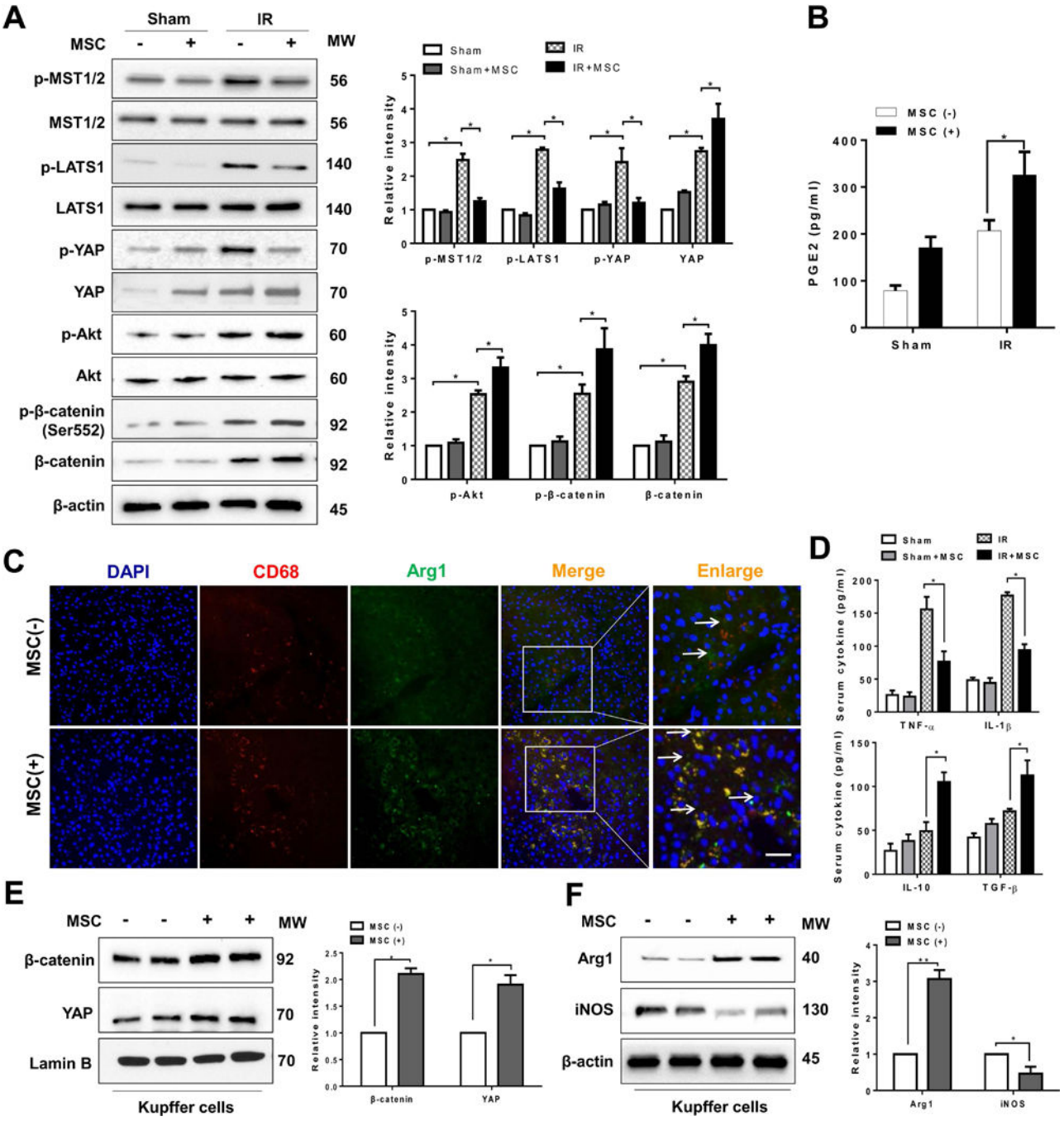

Figure 2. MSCs regulate Hippo signaling/β-catenin activation and control macrophage polarization in IR-stressed livers.

(A) Immunoblot-assisted analysis and relative density ratio of p-MST½, MST½, p-LATS1, LATS1, p-YAP, YAP, p-Akt, Akt, p-β-catenin, and β-catenin in IR-stressed livers with or without MSC treatment. Representative of three experiments. (B) ELISA analysis of PGE2 levels in animal serum (n=3–4 samples/group). (C) Representative immunofluorescence staining for the macrophage marker CD68 (red) and arginase-1 (Arg1, green) co-localization in IR-stressed livers (n=3–4 mice/group). DAPI was used to visualize nuclei (blue). Arrow indicated CD68 and Arg1 double positive macrophages (yellow). Scale bars, 20μm. (D)

ELISA analysis of TNF-α, IL-1β, IL-10, and TGF-β levels in animal serum (n=3–4 samples/group). Immunoblot-assisted analysis and relative density ratio of nuclear YAP and β-catenin (E), and Arg1 and iNOS (F) in liver Kupffer cells. Representative of three experiments. All data represent the mean±SD. *p<0.05, **p<0.01.

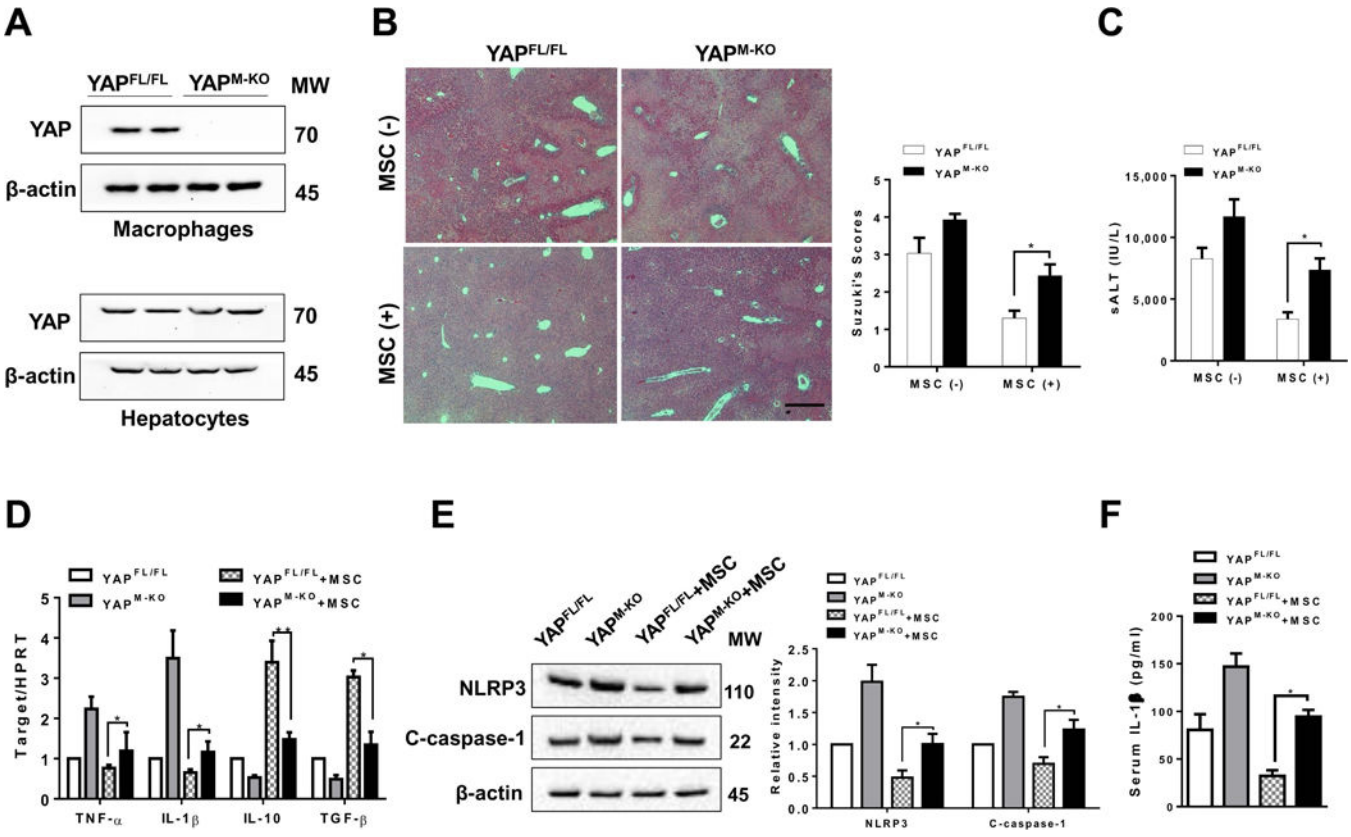

Figure 3. Myeloid YAP deficiency in MSC-treated livers aggravates IR-induced hepatocellular damage and promotes NLRP3 inflammasome-driven inflammatory response.

The $YAP^{FL/FL}$ and $YAP^{M\text{-}KO}$ mice were subjected to 90min of partial liver warm ischemia, followed by 6h of reperfusion. Some animals were injected via tail vein with MSCs (1×10^6) 24h prior to ischemia. (A) The YAP expression was detected in hepatocytes and liver macrophages (Kupffer cells) by Western blot assay. Representative of three experiments. (B) Representative histological staining (H&E) of ischemic liver tissue (n=4–6 mice/group) and Suzuki's histological score. Scale bars, 100μm. (C) Hepatocellular function was evaluated by sALT levels (IU/L) (n=4–6 samples/group). (D) qRT-PCR-assisted detection of TNF-α, IL-1β, IL-10, and TGF-β in ischemic livers (n=3–4 samples/group). Data were normalized to HPRT gene expression. (E) Immunoblot-assisted analysis and relative density ratio of NLRP3 and cleaved caspase-1 in ischemic livers. Representative of three experiments. (F) ELISA analysis of IL-1β levels in animal serum (n=3–4 samples/group). All data represent the mean±SD. *p<0.05, **p<0.01.

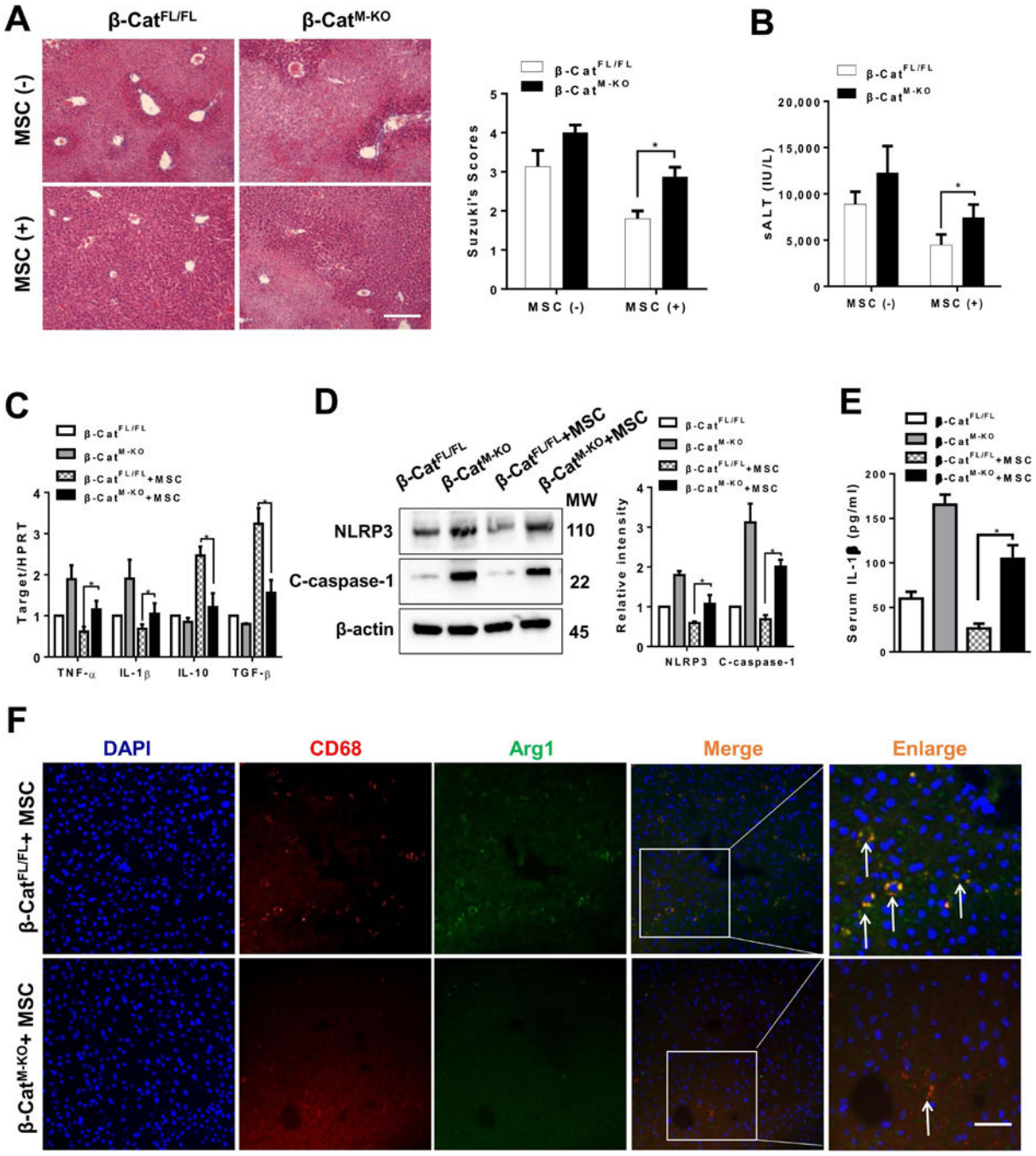

Figure 4. Disruption of myeloid β-catenin in MSC-treated livers activates NLRP3 and diminishes M2 macrophage polarization in IR-stressed livers.

The β-catenin$^{FL/FL}$ and β-catenin^{M-KO} mice were subjected to 90min of partial liver warm ischemia, followed by 6h of reperfusion. Some animals were injected via tail vein with MSCs (1×10^6) 24h prior to ischemia. (A) Representative histological staining (H&E) of ischemic liver tissue (n=4–6 mice/group) and Suzuki's histological score. Scale bars, 100μm. (B) Hepatocellular function was evaluated by sALT levels (IU/L) (n=4–6 samples/group). (C) qRT-PCR-assisted detection of TNF-α, IL-1β, IL-10, and TGF-β in ischemic livers (n=3–4 samples/group). Data were normalized to HPRT gene expression. (D)

Immunoblot-assisted analysis and relative density ratio of NLRP3 and cleaved caspase-1 in ischemic livers. Representative of three experiments. (E) ELISA analysis of IL-1β levels in animal serum (n=3–4 samples/group). (F) Representative immunofluorescence staining for the macrophage marker CD68 (red) and arginase-1 (Arg1, green) co-localization in IR-stressed livers (n=3–4 mice/group). DAPI was used to visualize nuclei (blue). Arrow indicated CD68 and Arg1 double positive macrophages (yellow). Scale bars, 20 μm. All data represent the mean±SD. *$p<0.05$.

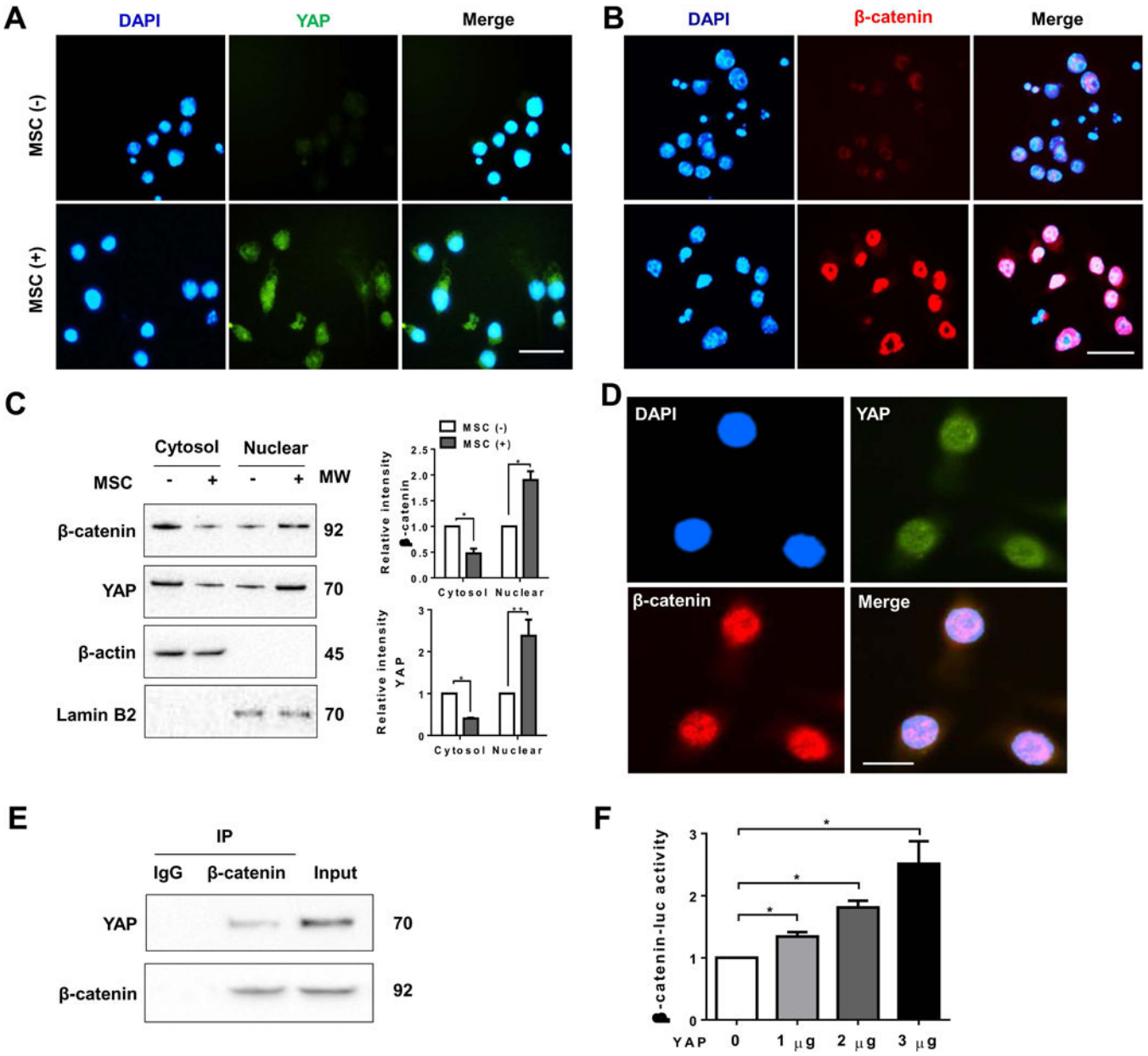

Figure 5. YAP interacts with β-catenin and regulates its transcription activity in MSC-mediated immune regulation.

Bone marrow-derived macrophages (BMMs, 1×10^6) were co-cultured with MSCs (2×10^5) for 24h followed by LPS (100 ng/ml) stimulation. (A) and (B) Immunofluorescence staining of nuclear YAP (green) and β-catenin (red) in macrophages after co-culture with or without MSCs. DAPI was used to visualize nuclei (blue). Scale bars, 20μm. (C) Immunoblot-assisted analysis of cytosol and nuclear YAP and β-catenin in macrophages after co-culture with or without MSCs. Representative of three experiments. (D) Immunofluorescence staining for macrophage YAP (green) and β-catenin (red) co-localization in the nucleus after co-culture with MSCs. DAPI was used to visualize nuclei (blue). Scale bars, 10μm. (E) Immunoprecipitation analysis of YAP and β-catenin in macrophages after co-culture with

MSCs. Representative of three experiments. (F) BMMs were co-transfected with 1μg β-catenin-luc and CRISPR YAP activation vectors. The luciferase activity was measured after 48h (n=3–4 samples/group). Data represent the mean±SD. *p<0.05.

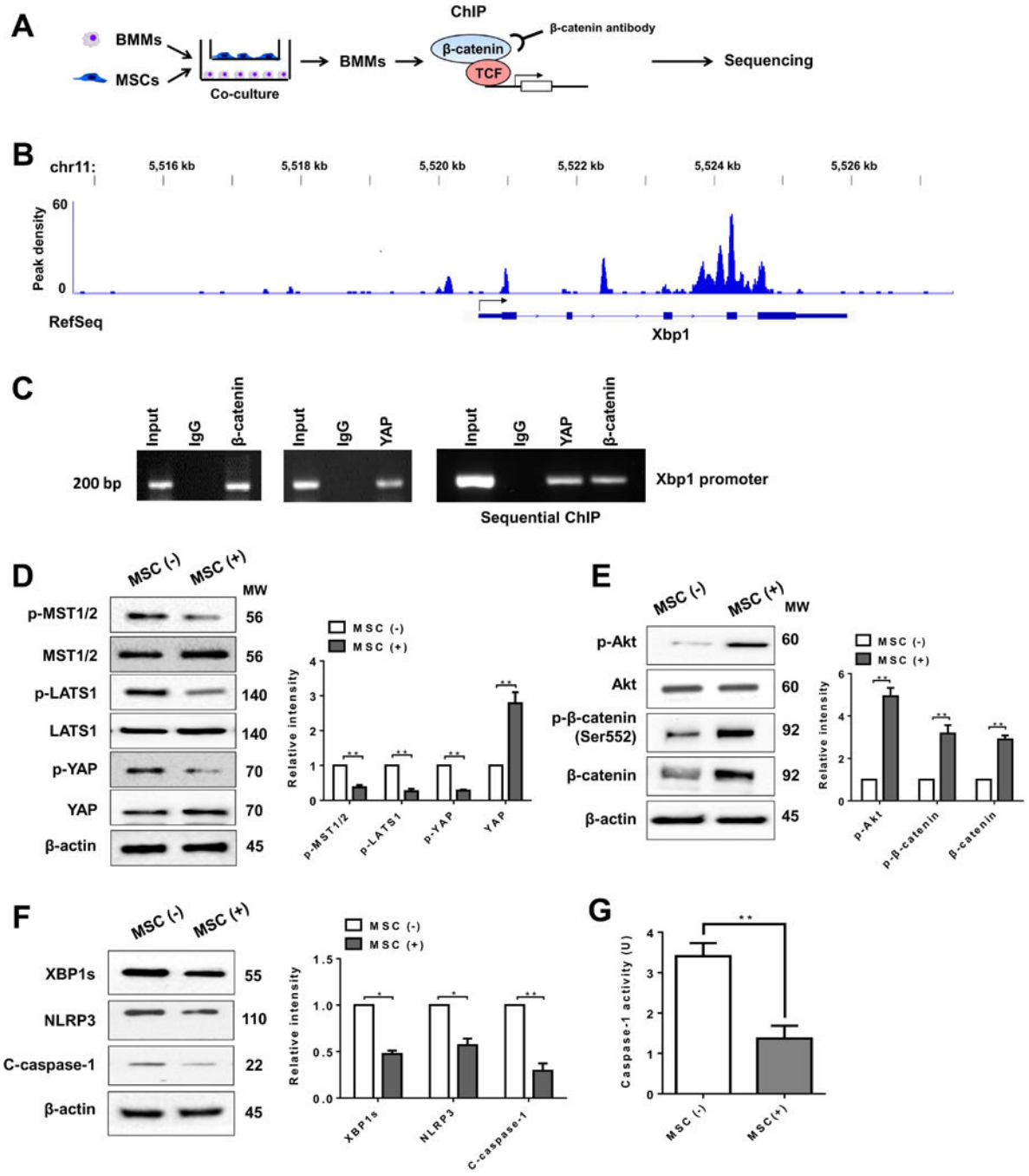

Figure 6. The YAP-β-catenin signaling targets XBP1 and inhibits NLRP3-driven inflammatory response in MSC-mediated immune regulation.

(A) Experimental design of β-catenin ChIP-seq analysis. BMMs were collected and fixed after co-culture with MSCs. Following chromatin shearing and β-catenin antibody selection, the precipitated DNA fragments bound by β-catenin-containing protein complexes were used for sequencing. (B) Localization of β-catenin-binding sites on the mouse *xbp1* gene. The five exons, four introns, 3' UTR, 5' UTR and TSS of the mouse *xbp1* gene on chromosome 11 are shown. (C) ChIP-PCR analysis of YAP and β-catenin binding to the Xbp1 promoter. Protein-bound chromatin was prepared from BMMs and

immunoprecipitated with YAP or β-catenin antibodies. For sequential ChIP, the protein-bound chromatin was first immunoprecipitated with the β-catenin antibody followed by elution with a second immunoprecipitation using YAP antibody, and then the immunoprecipitated DNA was analyzed by PCR. The normal IgG was used as a negative control. (D) (E) (F) Immunoblot-assisted analysis and relative density ratio of p-MST½, MST½, p-LATS1, LATS1, p-YAP, YAP, p-Akt, Akt, p-β-catenin, β-catenin, XBP1s, NLRP3, and cleaved caspase-1 in macrophages after co-culture with or without MSCs. Representative of three experiments. (G) Caspase-1 activity (U) in macrophages after co-culture (n=3–4 samples/group). All data represent the mean±SD. *p<0.05, **p<0.01.

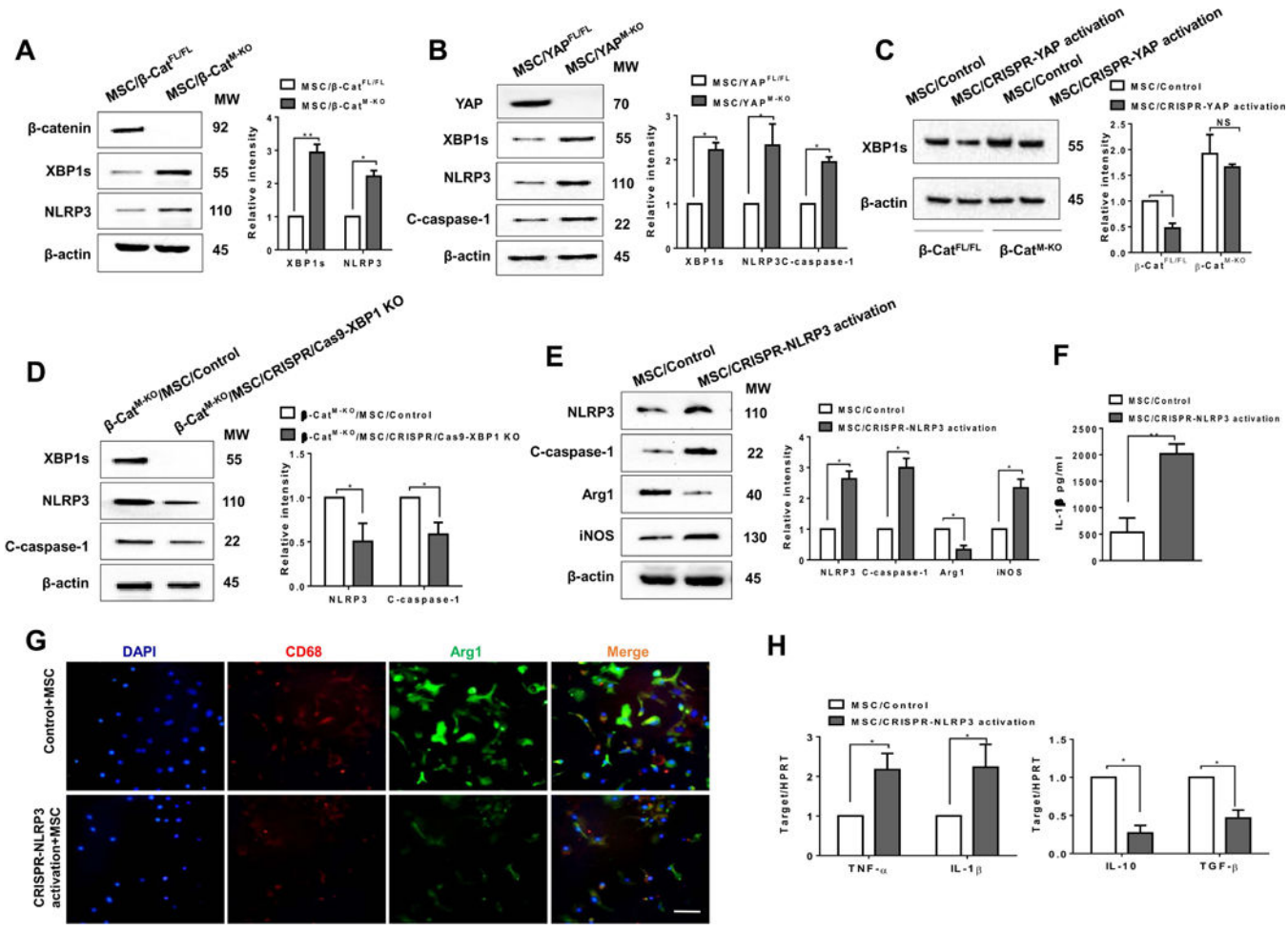

Figure 7. YAP is crucial to mediate β-catenin activity and reprograms NLRP3-dependent macrophage polarization in MSC-mediated immune regulation.

(A) (B) BMMs were isolated from β-catenin$^{FL/FL}$, β-catenin^{M-KO}, YAP$^{FL/FL}$, YAP^{M-KO} mice and then co-cultured with MSCs followed by LPS stimulation (n=3–4 samples/group). Immunoblot-assisted analysis and relative density ratio of macrophage β-catenin, YAP, XBP1s, and NLRP3, and cleaved caspase-1. Representative of three experiments. (C) BMMs were isolated from β-catenin$^{FL/FL}$ and β-catenin^{M-KO} mice and transfected with CRISPR-mediated YAP activation or control vector, and then co-cultured with MSCs followed by LPS stimulation. Immunoblot-assisted analysis and relative density ratio of macrophage XBP1s. Representative of three experiments. (D) BMMs were isolated from β-catenin^{M-KO} mice and transfected with CRISPR/Cas9-mediated XBP1 KO or control vector and then co-cultured with MSCs followed by LPS stimulation. Immunoblot-assisted analysis and relative density ratio of macrophage XBP1s, NLRP3, and cleaved caspase-1. Representative of three experiments. Fig. 7E-H, BMMs were isolated from β-catenin$^{FL/FL}$ mice and transfected with CRISPR-mediated NLRP3 activation or control vector were co-cultured with MSCs followed by LPS stimulation. (E) Immunoblot-assisted analysis and relative density ratio of macrophage NLRP3, cleaved caspase-1, Arg1, and iNOS. Representative of three experiments. (F) ELISA analysis of IL-1β levels in animal serum (n=3–4 samples/group). (G) Representative immunofluorescence staining for the

macrophage marker CD68 (red) and arginase-1 (Arg1, green) co-localization in BMMs. DAPI was used to visualize nuclei (blue). Scale bars, 20μm. (H) qRT-PCR-assisted detection of TNF-α, IL-1β, IL-10, and TGF-β in macrophages (n=3–4 samples/group). Data were normalized to HPRT gene expression. All data represent the mean±SD. *p<0.05, **p<0.01.

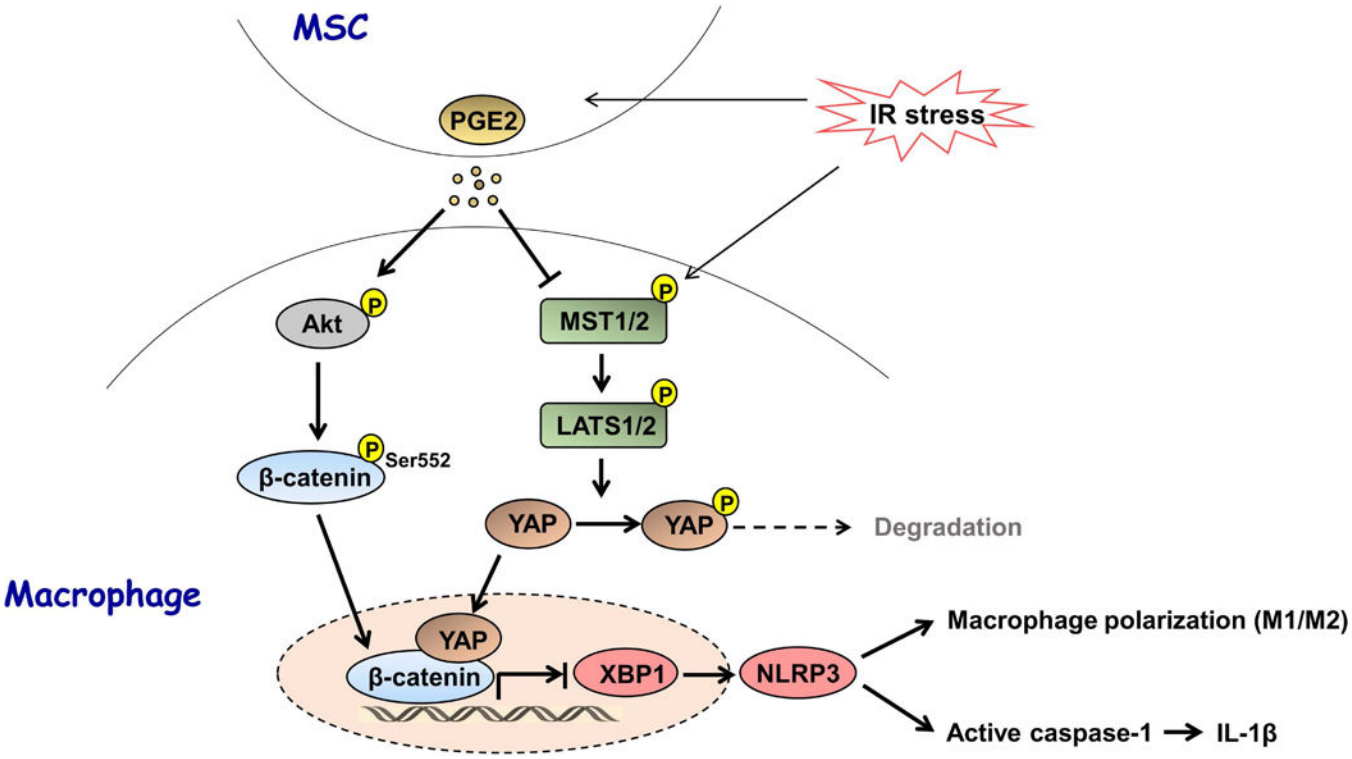

Figure 8. Schematic illustration how Hippo signaling may control NLRP3 activation in MSC-mediated immune regulation.

IR stress increases MSC-mediated PGE2 section, which in turn activates macrophage Akt and phosphorylates β-catenin at Ser552 leading to translocation of β-catenin into nucleus. Notably, MSCs regulate macrophage Hippo-YAP pathway by depressing MST½ and LATS1 phosphorylation, and increasing YAP translocation from cytoplasm to nucleus where YAP co-localizes and interacts with nuclear β-catenin, which in turn regulates their target gene XBP1 leading to reduced NLRP3/caspase-1 activity and IL-1β release, and augmented M2 macrophage phenotype in IR-triggered liver inflammation.